# Burial induced changes in physical sandstone properties: A case-study of North Sea and Norwegian Sea sandstone formations

*Lara A. Blazevic V.*, Kenneth Duffaut, and Per Avseth, Norwegian University of Science and Technology (NTNU)*

**Summary**

The changes in physical properties of sandstones with burial depth are a result of mechanical and chemical compaction processes. These processes are affected by rock microstructure, pressure regimes and temperature history. Data from 30 wells have been used to investigate and compare the changes in porosity, bulk density, elastic moduli and wave propagation velocities between mid-Jurassic sandstones in the North Sea and the Norwegian Sea. Mechanical compaction and quartz cementation models are used together with rock physics diagnostics to describe these changes.

**Introduction**

The physical properties of rocks are fundamental for the study of sedimentary basins and the characterization of hydrocarbon reservoirs. Properties such as porosity, bulk density and wave propagation velocities of the rock can be obtained or derived from well log data and they may provide information about rock composition and structure.

The properties of a formation change with depth due to compaction. The compaction processes drive the sediments towards higher mechanical and thermodynamic stability (Thyberg and Jahren, 2011). Mechanical compaction starts immediately after deposition and is governed by increasing net stress, generated from the weight of the overburden, resulting in volume reduction due to rearrangement or breaking of grains (Marcussen et al., 2010; Thyberg and Jahren, 2011). Chemical compaction is controlled by thermodynamics and involves dissolution and precipitation of solids; in sandstones, the most important type of chemical compaction is caused by the precipitation of quartz, which begins around 70-80°C (Ehrenberg, 1990; Walderhaug, 1994a).

The changes in physical properties with burial depth of two time equivalent sandstone formations from the North Sea (Etive Fm.) and the Norwegian Sea (Garn Fm.) are modeled and analyzed with information from 15 wells from each basin. To achieve this, the changes in porosity, bulk density, elastic moduli and wave propagation velocities are studied separately for the mechanical and chemical compaction domains. Combinations of Lander and Walderhaug's model (1999) and the friable-sand model, and of Walderhaug's model (1996) and the contact-cement model, are used to describe the changes in these physical properties in the mechanical compaction domain and in the chemical compaction domain, respectively.

We investigate how different factors related to rock microstructure, pressure regimes and temperature history can affect the mechanical and chemical compaction processes, and how the deviations from the trends can provide further information about these factors.

**Theory and Method**

Porosity Modeling

Lander and Walderhaug (1999) proposed a compaction function to explain the intergranular volume loss as a function of effective stress, given by:

$$IGV = IGV_f + (\phi_0 + m_0 - IGV_f)\, e^{-\beta \sigma_{es}} \quad (1)$$

where IGV is the sum of pore space, cements and matrix material, and $IGV_f$ is the stable packing configuration, both in volume fraction; $\phi_0$ is the depositional porosity (volume fraction), $m_0$ is the initial proportion of matrix material (volume fraction), $\beta$ is the exponential rate of IGV decline with effective stress ($MPa^{-1}$), and $\sigma_{es}$ is the maximum effective stress (in MPa, hydrostatic pressure is assumed).

This model was used to simulate the porosity loss due to mechanical compaction. From previous studies on core samples of the Etive and Garn formations (Ehrenberg, 1990; Marcussen et al., 2010), the values of $IGV_f$ were set to 0.28 and 0.26, respectively. We assumed a depositional porosity, $\phi_0$, of 0.40 and $m_0$ was set to 0; the sum of these two variables constitutes the initial IGV (i.e. IGV at zero effective stress). The value of $\beta$ was fixed to 0.06 $MPa^{-1}$, as that documented by Lander and Walderhaug (1999) to provide good correspondence between model predictions and measurements in sandstones.

To predict quartz cementation, Walderhaug (1996) estimated the volume of quartz cement, Vq (in $cm^3$), that precipitated in a 1 $cm^3$ volume of sandstone with quartz surface area A (in $cm^2$) during time t (in s), as:

$$Vq = MrAt/\rho \quad (2)$$

where M is the molar mass of quartz (60.09 g/mole), r is the quartz precipitation rate (in moles/$cm^2$s), and $\rho$ is the

density of quartz (2.65 g/cm$^3$). The quartz precipitation rate is dependent on temperature, while the quartz surface area is dependent on grain size, fraction of quartz and clay coatings. At any time, the porosity is given by the porosity at the onset of quartz cementation minus the volume of quartz cement at that given time.

Quartz cementation was simulated by means of this model. The temperature at the start of quartz cementation was set to 75°C, corresponding to about 2 km burial depth in the studied areas in accordance with bottom hole temperature data, which was also consistent with previous authors observations (Ehrenberg, 1990; Storvoll et al., 2005; Marcussen et al., 2010). The fraction of detrital quartz was set to 0.65 based on Marcussen et al. (2010) petrographic analysis. The clay coating was assumed to be 0.1. Grain sizes varied between 0.2-0.6 mm for the Etive sandstones (Marcussen et al., 2010), and between 0.2-0.4 mm for the Garn sandstones (Ehrenberg, 1990). Temperature and burial history curves for each formation (Walderhaug, 1994b) were used to derive temperature increase rates and to express the porosity loss (quartz cementation) as a function of depth.

For this study we focused on "clean" sandstones with less than 5% clay. The clay volume was computed as an average of clay volume from gamma ray log and clay volume from neutron-density logs. Considering that several of the studied wells contained gas or condensate, the porosity was estimated from density-neutron logs. The aim of this approach was to reduce uncertainties related to the unknown fluid density. The resulting porosity loss trends from the mechanical compaction and quartz cementation models were compared with the data derived from the wells (Figure 1).

Elastic Moduli and Velocities Modeling

The models derived from the rock physics diagnostics technique, introduced by Dvorkin and Nur (1996), allow us to relate the elastic moduli of sediments and rocks to their porosity for different rock and sediment microstructures. Two models were presented: the friable-sand model and the contact-cement model.

The friable-sand model, or the unconsolidated line, describes the elastic moduli-porosity relation when sorting deteriorates (Avseth et al., 2010). The dry elastic moduli of the well-sorted end point at critical porosity are given by the Hertz-Mindlin theory. At zero porosity, the elastic dry moduli correspond to those of the mineral. The moduli of poorly sorted sands with porosities between zero and critical porosity are interpolated between the mineral point and the well sorted point by means of Hashin-Strikman lower bound.

In contrast, the contact-cement model assumes that porosity reduces from the initial porosity of a sand pack as result of the uniform deposition of cement on the surface of the grain (Avseth et al., 2010).

A combination of the friable-sand and contact-cement models was used to model the diagenesis processes after deposition (Figure 2). Following Gassmann's fluid substitution for the bulk modulus, P- and S-wave velocities at 100% water saturation were estimated and also modeled.

From the well log data, water saturation in the formations of interest was computed from Archie's equation (1952). Most of the studied wells contained hydrocarbons, either gas or oil, or a combination of both. The densities and the bulk moduli of the involved fluids were calculated following Batzle and Wang's (1992) calculations.

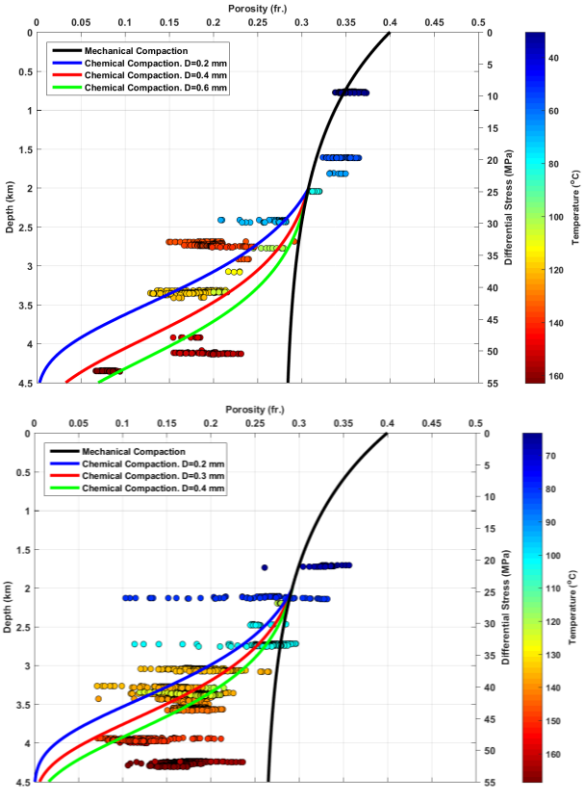


Figure 1: Porosity-depth trends in the mechanical and chemical compaction domains for the sandstones of the Etive Fm. (top) and the Garn Fm. (bottom). The data is color-coded by formation temperature. The depth is given as true vertical depth measured from sea floor. D = grain size.

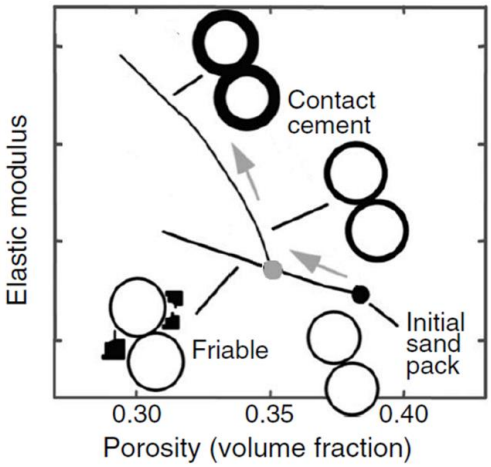


Figure 2: Schematic of the combination of the friable-sand and contact-cement models to follow the diagenetic processes after deposition. (Modified from Avseth et al., 2010).

To perform a sensible comparison and correlation with the data from all the wells, fluid substitution to a 100% water saturated scenario was carried out for the wells with hydrocarbon content. The fluid substitution was performed following Mavko et al. (1995) approximation of the Gassmann's relation for the P-wave modulus, given that S-wave velocity logs were not available. Without S-wave velocity measurements, the shear modulus of the formations remains unknown, and therefore, the bulk modulus of the saturated rock in situ cannot be estimated. After obtaining the P-wave velocity at 100% water saturation, the S-wave velocity for the same scenario was estimated from Greenberg and Castagna's relation (1992). Knowing the P-wave and shear moduli we then estimated the bulk modulus.

Figures 3 and 4 show the dry bulk modulus and the 100% water saturated P-wave velocity of the Etive and Garn formations, respectively. The data is plotted together with the combination of the friable-sand and contact-cement models. These models were converted to a depth domain from the porosity-depth relationships shown in Figure 1, and they are plotted together with the data in Figure 5.

**Discussion of Results/Conclusions**

In both the Etive Fm. and Garn Fm. the changes in physical properties with burial depth result from two different compaction processes: mechanical compaction and chemical compaction.

The mechanical compaction governs up to about 2 km burial depth, corresponding to temperatures around 75°C. The general underprediction of porosity values for the shallower sandstones (< 2 km burial depth) by the mechanical compaction model suggests that both Etive and Garn Fm. have high depositional porosities (> 0.40). On the other hand, the model's underprediction of dry bulk modulus and P-wave velocity in the same sandstones (at 1.6-2.0 km burial depth) suggests that these might be slightly cemented, with little amounts of quartz cement stiffening the rocks but not affecting their porosities significantly.

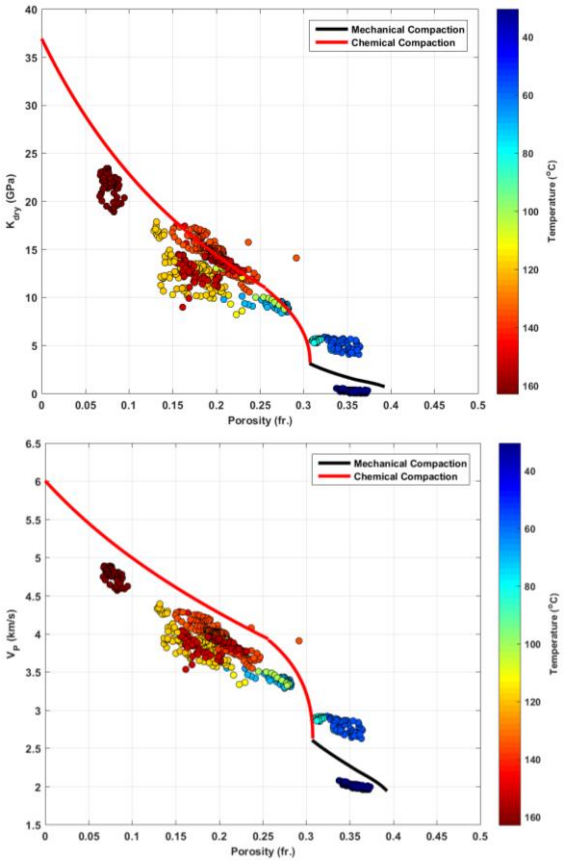


Figure 3: Dry bulk modulus (top) and P-wave velocity at 100% water saturation (bottom) versus porosity for the Etive Fm. with compaction models.

At burial depths greater than 2 km, chemical compaction is the main controlling process in the changes of physical properties. The greater variations in porosity values for the Garn sandstones at the same depth suggest that they are less well sorted than the Etive sandstones, and that the quartz cement also distributes less evenly. For both formations, there is a steep decrease in porosity from 2-3.5 km burial depth, and at greater depths there is, generally, no further significant reduction in porosity values. These high porosities at great burial depths (> 4 km) suggest the

presence of significant amounts of clay coatings inhibiting the quartz cementation. The well completion reports state high overpressures in these sandstones, indicating that the porosity preservation might also be influenced by low effective stresses.

In the dry bulk modulus-porosity domain, the greater variations in bulk modulus values for Garn sandstones with the same porosity may suggest that they are more affected by different quartz deposition distributions than the Etive sandstones.

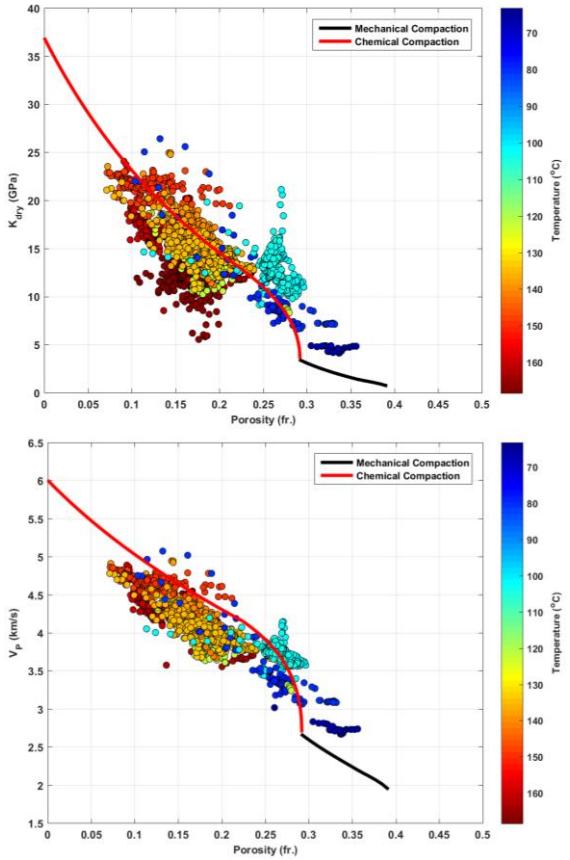


Figure 4: Dry bulk modulus (top) and P-wave velocity at 100% water saturation (bottom) versus porosity for the Garn Fm. with compaction models.

From the general overpredictions of dry elastic moduli and velocities at greater burial depths, it is recommended to use or develop models that take into account the effects of varying effective stresses in the chemical compaction domain (e.g., Vernik and Kachanov, 2010). Cracks can occur at greater depths, which are not modeled with the contact cement model and can cause variability in elastic moduli and velocities. Avseth et al. (2014) used the differential effective medium to capture cracks at greater depths. At the presence of overpressure, the cracks will open and have a larger effect on velocities.

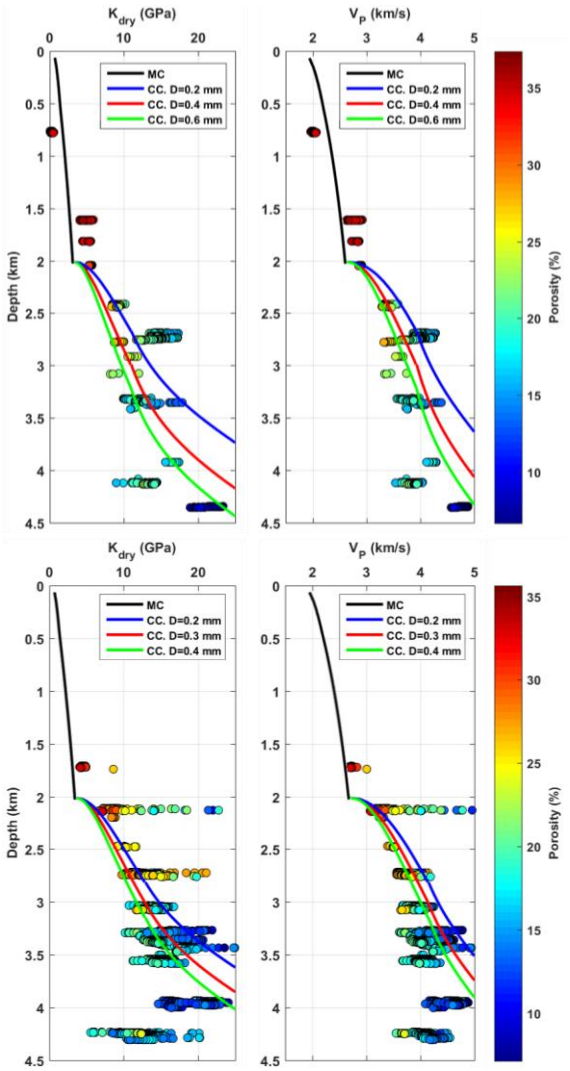


Figure 5: Dry bulk modulus and P-wave velocity (Sw=100%) versus depth for the Etive Fm. (top) and the Garn Fm. (bottom) with compaction models. The data is color-coded by formation temperature.

**Acknowledgments**

We would like to thank NTNU for supporting this study, and the Norwegian Petroleum Directorate and Schlumberger for providing the data. Thanks to Ivan Lehocki for helpful discussions and suggestions.

**EDITED REFERENCES**

Note: This reference list is a copyedited version of the reference list submitted by the author. Reference lists for the 2017 SEG Technical Program Expanded Abstracts have been copyedited so that references provided with the online metadata for each paper will achieve a high degree of linking to cited sources that appear on the Web.

**REFERENCES**


Archie, G. E., 1952, Classification of carbonate reservoir rocks and petrophysical considerations: AAPG Bulletin, **36**, 278–298, https://doi.org/10.1306/3d9343f7-16b1-11d7-8645000102c1865d.

Avseth, P., T. A. Johansen, A. Bakhorji, and H. M. Mustafa, 2014, Rock-physics modeling guided by depositional and burial history in low-to-intermediate-porosity sandstones: Geophysics, **79**, no. 2, D115–D121, http://doi.org/10.1190/geo2013-0226.1.

Avseth, P., T. Mukerji, G. Mavko, and J. Dvorkin, 2010, Rock-physics diagnostics of depositional texture, diagenetic alterations, and reservoir heterogeneity in high-porosity siliciclastic sediments and rocks—A review of selected models and suggested work flows: Geophysics, **75**, no. 5, 75A31–75A47, https://doi.org/10.1190/1.3483770.

Batzle, M., and Z. Wang, 1992, Seismic properties of pore fluids: Geophysics, **57**, 1396–1408, https://doi.org/10.1190/1.1443207.

Dvorkin, J., and A. Nur, 1996, Elasticity of high-porosity sandstones: Theory for two North Sea data sets: Geophysics, **61**, 1363–1370, https://doi.org/10.1190/1.1444059.

Ehrenberg, S. N., 1990, Relationship between diagenesis and reservoir quality in sandstones of the Garn Formation, Haltenbanken, mid-Norwegian continental shelf: AAPG Bulletin, **74**, 1538–1558, https://doi.org/10.1306/0c9b2515-1710-11d7-8645000102c1865d.

Greenberg, M. L., and J. P. Castagna, 1992, Shear-wave velocity estimation in porous rocks: Theoretical formulation, preliminary verification and applications: Geophysical Prospecting, **40**, 195–209, http://doi.org/10.1111/j.1365-2478.1992.tb00371.x.

Lander, R. H., and O. Walderhaug, 1999, Predicting porosity through simulating sandstone compaction and quartz cementation: AAPG Bulletin, **83**, 433–449, https://doi.org/10.1306/00aa9bc4-1730-11d7-8645000102c1865d.

Marcussen, Ø., T. E. Maast, N. H. Mondol, J. Jahren, and K. Bjørlykke, 2010, Changes in physical properties of a reservoir sandstone as a function of burial depth–The Etive Formation, northern North Sea: Marine and Petroleum Geology, **27**, 1725–1735, https://doi.org/10.1016/j.marpetgeo.2009.11.007.

Mavko, G., C. Chan, and T. Mukerji, 1995, Fluid substitution: Estimating changes in Vp without knowing Vs: Geophysics, **60**, 1750–1755, https://doi.org/10.1190/1.1443908.

Storvoll, V., K. Bjørlykke, and N. H. Mondol, 2005, Velocity-depth trends in Mesozoic and Cenozoic sediments from the Norwegian Shelf: AAPG Bulletin, **89**, 359–381, http://doi.org/10.1306/10150404033.

Thyberg, B., and J. Jahren, 2011, Quartz cementation in mudstones: Sheet-like quartz cement from clay mineral reactions during burial: Petroleum Geoscience, **17**, 53–63, https://doi.org/10.1144/1354-079310-028.

Vernik, L., and M. Kachanov, 2010, Modeling elastic properties of siliciclastic rocks: Geophysics, **75**, no. 6, E171–E182, https://doi.org/10.1190/1.3494031.

Walderhaug, O., 1994a, Precipitation rates for quartz cement in sandstones determined by fluid-inclusion microthermometry and temperature-history modeling: Journal of Sedimentary Research, **64**, 324–333, https://doi.org/10.2110/jsr.64.324.

Walderhaug, O., 1994b, Temperatures of quartz cementation in Jurassic sandstones from the Norwegian continental shelf—Evidence from fluid inclusions: Journal of Sedimentary Research, **64**, 311–323, http://doi.org/10.1306/D4267D89-2B26-11D7-8648000102C1865D.

Walderhaug, O., 1996, Kinetic modeling of quartz cementation and porosity loss in deeply buried sandstone reservoirs: AAPG Bulletin, **80**, 731–745, https://doi.org/10.1306/64ed88a4-1724-11d7-8645000102c1865d.